Modeling Neuronal Nicotinic and GABA Receptors: Important Interface Salt-Links and Protein Dynamics

Richard J. Law and Felice C. Lightstone*
Biosciences and Biotechnology Division, Physical and Life Sciences Directorate, Lawrence Livermore National Laboratory, Livermore, California

ABSTRACT Protein motions in the Cys-loop ligand-gated ion receptors that govern the gating mechanism are still not well understood. The details as to how motions in the ligand-binding domain are translated to the transmembrane domain and how subunit rotations are linked to bring about the cooperative movements involved in gating are under investigation. Homology models of the $\alpha4\beta2$ nicotinic acetylcholine (nACh) and $\beta2\alpha1\gamma2$ GABA receptors were constructed based on the torpedo neuromuscular-like nicotinic receptor structure. The template constructed for the full electron microscopy structure must be considered more reliable for structure-function studies due to the preservation of the E45–R209 salt-link. Many other salt-links are seen to transiently form, including switching off of the E45–R209 link, within a network of potential salt-links at the binding domain to the transmembrane domain interface region. Several potentially important intersubunit salt-links form in both the nAChR and GABAR structures during the simulation and appear conserved across many subunit combinations, such as the salt-link between α4.E262 and β2.K255 in nAChR (β2.E262 and α1.K263 in GABAR), at the top of the pore-lining M2 helices, and the intersubunit link of R210 on the M1-linker to E168 on the β8-sheet of the adjacent subunit in the GABA receptor (E175–K46 being the structurally equivalent link in the nAChR, with reversed polarity). A network of other salt-links may be vital for transmitting the cooperative gating motions between subunits that become biased upon ligand binding. The changes seen in the simulations suggest that this network of salt-links helps to set limits and specific states for the conformational changes involved in gating of the receptor. We hope that these hypotheses will be tested experimentally in the near future.

INTRODUCTION

The γ-aminobutyric acid (GABA) and nicotinic acetylcholine (nACh) receptors are two members of the Cys-loop ligand-gated ion channel (CL-LGIC) family. Other members of this family include glycine and serotonin (5-HT_3) receptors (1). This family of channels has been implicated in numerous diseases and conditions, ranging from schizophrenia to drug addiction (2). The nACh receptor (nAChR) channels represent a major excitory cation channel in the brain and throughout the body. The channels are formed from the pentameric arrangement of various monomer subtypes: α, β, γ, δ, and ε. At least two α-subunits must be present because they always comprise one face of the two required agonist-binding sites, as well as the C-loop that encloses the site, which sits at the interface between α- and another subunit. The major inhibitory receptor in the brain is the GABA receptor (GABAR) chloride channel (3). It includes two pharmacological forms—$GABA_A$ and $GABA_C$—that are differentiated by their sensitivity to bicuculline and many other compounds, such as barbituates and benzodiazepines (4). The dominant $GABA_A$ form is formed from a mix of α-, β-, γ-, δ-, ε-, θ-, and Π- subunit types. $GABA_C$ receptors are comprised solely of bicuculline-insensitive ρ-subunits; however, some mixing of GABAR α-, γ-, and ρ-subtypes has been observed (5). In the case of GABAR, it is the β-subunit that plays the vital agonist-binding site role. For this study, the major neuronal subtypes of GABAR and nAChR were chosen both because of their overwhelming presence on synapses in the brain, and because of the experimental evidence supporting their important interactions with allosteric effectors molecules. For GABAR this is the $\beta2_{(2)}\alpha1_{(2)}\gamma2$ form, whereas for nAChR it is the $\alpha4_{(2)}\beta2_{(3)}$ oligomer. The stoichiometric arrangement of these channels has been established (6).

In each case (and for all CL-LGICs other than the homomeric forms, such nAChR α7), there are two binding sites for the natural agonist, i.e., acetylcholine or GABA. The agonist-binding site sits at the interface between subunits. In the case of nAChRs, the α-subunits always form the so-called +-side (left face) of the binding site, providing the overlapping C-loop. Functionally, then, this is equivalent to the β-subunits in the GABARs (6,7). Other ligands may bind at other subunit interfaces, such as benzodiazepines and barbiturates, which bind at the α-γ interface in GABAR, and noncompetitive antagonists, such as cocaine and galanthamine, may also bind at interfaces in the ligand-binding domain (LBD) other than the agonist-binding site (8,9). Many noncompetitive antagonists and agonists of CL-LGICs are known to interact with the transmembrane domain (TMD) without necessarily directly blocking the pore, such as tetracaine (10), ketamine (both anesthetics) (11), a series of antidepressants (12), and various steroids (13).

In any structural investigation involving homology modeling and molecular-dynamics (MD) simulation, template selection is vitally important. The template must have sufficiently high resolution to represent accurately enough the

Submitted May 16, 2008, and accepted for publication June 11, 2009.

*Correspondence: felice@llnl.gov

Richard J. Law's present address is 114 Milton Park, Abingdon, Oxfordshire, OX14 4SA, UK.

Editor: Edward H. Egelman.

0006-3495/09/09/1586/9 $2.00

doi: 10.1016/j.bpj.2009.06.044

interactions of the residues within the structure. Homology modeling and short MD can in fact improve the quality of some medium-resolution (>3Å) structures (14–16). The ''twist-to-open'' mechanism is currently favored (17,18) as a means of opening the narrow hydrophobic pore through which hydrated ions can flow through the receptor (19,20). However, the details of this mechanism are still being resolved. Multiple pathways exist within the protein for binding of the agonist to affect motion within the LBD, which then subsequently affects motion in the TMD (18). Multiple loops, secondary structure elements, and residue pairs have been shown to be potentially important in the transmission of this signal (22–25). Several recent works used homology models of CL-LGICs for simulation studies (26–28). The models support a ''twist-to-open'' mechanism of action that involves contact of the C-loop with the ligand binding at the agonist-binding site, which pulls on the $\beta 9\beta 10$ sheets, and its connection to the M1 helix on the TMD, enabling opening of the channel via the asymmetric outward motion and 10° rotation of the subunits. In this study, we analyze new models of the CL-LGIC family, test the relative accuracy of the templates for these models, and examine the protein dynamics to gain further information about the mechanism of the channel.

MATERIALS AND METHODS

Receptor modeling

A multiple sequence alignment of 40 CL-LGIC subunits plus the acetylcholine-binding protein (AChBP) was constructed using PSI-BLAST to obtain the sequences and ClustalW to create the multiple alignment once the sequences were selected (see Supporting Material). The homology model was based on two template structures: a chimera of the AChBP protein (Protein Data Bank (PDB): 1I9B) (29) and the TM-only electron microscopy (EM) structure of the *Torpedo californicans* nAChR (PDB: 1OED) (30). The second template used was the whole nAChR structure from *Torpedo marmorata* (PDB: 2BG9) (17), which includes the BD, TMD, and a portion of the vestibule domain.

The major neuronal forms of nAChR and GABAR—the $\alpha 4_{(2)}\beta 2_{(3)}$ nAChR and $\beta 2_{(2)}\alpha 1_{(2)}\gamma 2_{(1)}$ GABAR—with the most accepted subunit arrangement and stoichiometry for these forms (6), were chosen for this study. The β-subunits in GABARs are required for ligand-binding/gating, and they are therefore equivalent to the α-subunits in the nAChR for the purposes of the modeling required in this study. Also, due to the relative arrangement of the subunits, the GABA γ-subunit was modeled on the template β-subunit. Along with selection of each sequence as aligned with AChBP for use with the 1I9B-1OED chimeric template, four separate pairwise alignments were required as input for each full homology model based on the whole 2BG9 template and the TMD of the chimera-based models, as established by the equivalence of these subunits to those in the *T. marmorata* (*Tm*) sequences:

For $\alpha 4\beta 2$ nAChR

$$-Tm.\text{-}\alpha \rightarrow \text{n-}\alpha 4$$

$$-Tm.\text{-}\beta \rightarrow \text{n-}\beta 2$$

$$-Tm.\text{-}\delta \rightarrow \text{n-}\beta 2$$

$$-Tm.\text{-}\gamma \rightarrow \text{n-}\beta 2$$

For $\alpha 1\beta 2\gamma 2$ GABAR

$$-Tm.\text{-}\alpha \rightarrow g\text{-}\beta\alpha$$

$$-Tm.\text{-}\gamma \rightarrow g\text{-}\alpha 1$$

$$-Tm.\text{-}\beta \rightarrow g\text{-}\gamma 2$$

$$-Tm.\text{-}\delta \rightarrow g\text{-}\alpha 1$$

The constructed alignments were checked versus available data concerning equivalent or important residues both for nAChRs and GABARs (31,32). These were also compared with some other data for glycine and 5-HT3 receptors, the other two members of the CL-LGIC family (25).

A total of four models were constructed, in the closed/desensitized state of each: two human $\alpha 4_{(2)}\beta 2_{(3)}$ nAChR models (one based on the chimeric template and one based on the whole nAChR template) and two human $\beta 2_{(2)}\alpha 1_{(2)}\gamma 2$ $GABA_A$ receptor models (one based on the chimeric template and one based on the whole nAChR template). The missing loops in the 2BG9 structure were modeled when necessary and the complete receptor was modeled using MODELLER (33), without symmetry restraints, for each of the subunit pairwise alignments described above, extracted from the multiple alignment.

MD simulation

Here we describe a total of 60 ns of MD simulations of four 230,000 atom systems. All MD simulations were run using the CHARMM force field (34) (v27 for lipid and protein) in NAMD (35) with a nonbonded vdw cutoff of 9 Å. Four 15 ns simulations of the models inserted into an ionized, solvated lipid bilayer were performed.

An initial 110 × 110Å POPC (palmitoyl-2-oleoyl-sn-glycerol-phosphatidylcholine) bilayer slab, with water molecules positioned to hydrate the headgroups, was created using the Membrane package in VMD (36). This preliminary bilayer (consisting of 326 POPC molecules (163 in each leaflet) and 5529 water molecules) was then relaxed by steepest-descent minimization for 100 steps and equilibrated in MD for 500 ps to optimize the lipid-lipid and lipid-water packing.

The GABAR/nAChR model was then inserted into the center of the bilayer and all overlapping lipids and waters were removed. The aromatic girdle residues were lined up with the plane of the membrane. Each system was then fully solvated to a box size of 110 Å × 110 Å × 140 Å using Solvate (37). Enough Na^+ and Cl^- counterions were added to neutralize the charge on the protein and obtain a 0.15 M solution. The system was relaxed for 100 steps followed by a 500 ps equilibration MD run, with the positions of the heavy atoms of the protein restrained to their initial positions throughout. During the equilibration, the temperature was raised from 10 to 310 K under constant pressure conditions. This restrained run allowed the water and lipid to relax around the protein. Production simulations (i.e., those performed after minimization and equilibration) were conducted at constant pressure (NPT). Constant pressure was maintained with a Langevin piston set at 1 atm. Particle mesh Ewald electrostatics settings were applied to each system. All of the simulations were run with SHAKE (38) and with a 2-fs time step. TIP3P water (39) was used. Production runs (15 ns) were conducted at 310 K and maintained using a Langevin temperature piston. All of the MD runs were conducted on 512 processors of either MCR or Thunder machines at the Livermore Computing Center (MCR is a 2304 processor Intel Xeon machine, and Thunder is a 4096 Itanium II processor machine). Preparation, visualization, and analysis were performed on a Polywell AMD64 Dual processor machine running Red Hat Linux. Images were prepared and analysis was done using HOLE (40), Gromacs (41), Pymol (42), and VMD (36) with tcl/tk scripts.

RESULTS AND DISCUSSION

Four models (of two CL-LGICs) were examined to determine which template is best for further investigation of the proteins, or whether both are sufficient, and what underlying dynamical principles might govern the operation of these channels. It was found that to properly describe important pairwise interactions of residues at the BD and TMD interface, it is necessary to use the models derived from the 2BG9 EM structure of the full receptor (the full-EM template). Important salt-links in this region may allow gating to occur as they switch between forming BD to TMD links to forming links within the same domain, especially with respect to the important E45–R209 salt-link. In accordance with the above-mentioned ''twist-to-open'' mechanism, domain and subunit motions alter the spatial arrangement of residues at the domain and subunit interfaces, and altogether are suggestive of a mechanism whereby large-scale motions of the receptor are finely tuned and specifically limited by a network of salt-links at these interfaces.

Protein dynamics and template differences

We had to consider two important factors in determining which of the two available templates would best allow biologically relevant information to be extracted from the comparative simulations: 1) structural/experimental data that might differentiate between structures, and 2) the stability and quality of the model in simulation. The quality of the template structure is vitally important in homology modeling (14), as is the quality of the multiple alignment used to construct the pairwise alignment involved in construction of the model. In this study, two templates were used to produce four models: 2 $\alpha4_{(2)}\beta2_{(3)}$ nAChR structures, and two $\beta2_{(2)}\alpha1_{(2)}\gamma2$ GABAR models. The first template came from a chimera of two available structures: AChBP (PDB: 1I9B) (29) from the *Lymnaea stagnalis* pond snail, and the TMD of the *T. californicans* electric organ nAChR (PDB: 1OED) (30). The second template used was the almost complete receptor structure from *T. marmorata* (PDB: 2BG9) (17).

A comparison of the root mean-square deviation (RMSD) of models built from the two templates (shown for nAChR in Fig. 1 *A*, but similar for the GABAR models), indicates that the model built from the full-EM structure (2BG9) showed greater drift from the starting structure over the course of the 15 ns simulation. The initial RMSD observed in the simulations is due to relaxation of the structures. The secondary structure (Definition of Secondary Structure of Proteins (DSSP)) analysis revealed that this increased RMSD was due to two regions of the models, derived from the full-EM template, showing large fluctuations in the simulation (Fig. 1 *B*). MD simulations of the models resulting from the full-EM template had large motions in the peripheral BD helix. This can be seen in the DSSP plot for a nicotinic α-subunit (Fig. 1 *B*). In a comparison of the BD from the two templates, the BD is more extended in the full-EM model, and this peripheral helix is not as well packed against the top of the domain as it is in the AChBP chimeric model. It is not known what the role of this helix might be; however, a small number of residues that could act to stabilize this unit, if they were present in the structure, are missing from the N-terminus. Even more considerable motion of the vestibule helix was observed in the full-EM template-derived model of nAChR (Fig. 1 *B*). This is only a partially solved structure of this region of the protein

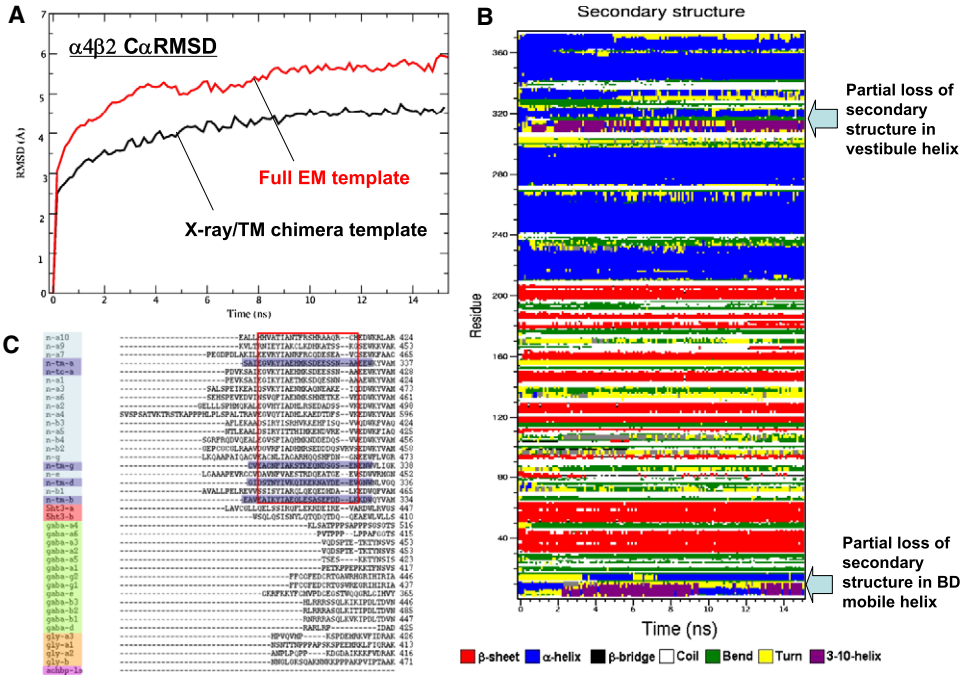

FIGURE 1 (*A*) RMSD for Cα atoms in the $\alpha4\beta2$ nAChR model simulations, demonstrating the difference in mobility between the two models. This added mobility is almost completely due to two small regions of the complex, as shown in *B*. This DSSP plot shows the mobility and loss of secondary structure in the vestibule helix and the peripheral binding domain helix. The vestibule helix was not present in the chimeric template, and therefore does not contribute to the RMSD. (*C*) Plot of the RMSF, averaged over five subunits, of the $\alpha4\beta2$ full-EM template model in simulation. The inset is an image of a single subunit of the channel structure, with the ribbons colored based on these RMSF values. It shows three ''hot'' areas: the binding domain helix, the C-loop, and the vestibule segment/domain.

(17), which somewhat explains its instability. This helix was not included in the GABAR models, as both the multiple alignment and secondary-structure prediction (Fig. 1 *C*) showed no evidence that this vestibule helix was conserved beyond the nicotinic acetylcholine branch of the CL-LGIC family. By plotting the root mean-square fluctuations (RMSFs), as shown in Fig. 2, we can see that the total RMSD values for the full-EM $\alpha4\beta2$ structure are dominated by three highly mobile regions of the structure: the BD helix, the C-loop, and the vestibule domain.

Template selection: important BD and TMD interface intrasubunit salt-links

As we describe the specific interactions taking place, each residue number will be preceded by the subunit identity and an ''n-'' when referring to the nAChR receptor, and a ''g-'' when referring to the GABA-A receptor. For example, ''n-β2-K255'' is lysine 255 in the $\beta2$ subunit of the nAChR. In cases involving multiple subunits, this will be expressed. The residue numbering refers to numbering within an alignment of the six different subunits investigated and is illustrated in Fig. 3. This more clearly allows a comparison between the different subunits and the two receptors.

A major consideration in template selection has to be the available experimental data. The interface between the BD and TMD is of major importance to channel function (43). A salt-link between R209 (on the $\beta10$–M1 linker) and E45 ($\beta1$–$\beta2$ loop) has been shown to be vital for gating dynamics (23) in the nAChR, as is the equivalent arginine in GABARs (32). These conserved residues are present in all subunits other than the GABA $\gamma2$ subunit, where the glutamate is an alanine (also, E45 = g-α1-D45). This link was not restrained in the initial modeling with either template. Twenty-three potential intrasubunit salt-bridges were identified within each subunit of the $\alpha4\beta2$ model based on the chimeric template, yet E45–R209 was not one of them. Most importantly, the E45–R209 salt-link was present throughout the simulations involving the models from the full-EM template (both nicotinic $\alpha4\beta2$ and GABAR), but was not present from the beginning of the simulations. For both the nicotinic and the GABAR models based on the chimeric template (Fig. 2), the E45–R209 salt link is not present from the initial modeling and does not form during the entire simulation. Instead, E45 transiently links to n-α4-K46/n-β2-R46 or g-β2-R135, and n-β2-R209 forms a link to n-β2-E175 on the $\beta8$–$\beta9$ loop. The difference in the starting orientation of the side chains, as well as the relatively more intervening position of the M2–M3 loop in the chimera-based models, discourages formation of the E45–R209 salt-link. This observation highlights a larger issue, i.e., that the interface between the BD and TMD is vitally important for the functional dynamics of the protein (43). The E45–R209 link is in fact the only consistent salt-bridge between the BD and TMD in the α-subunit of the nicotinic $\alpha4\beta2$ model simulation, even though several ionizable side chains exist in this area (25). All of the interface salt-links, including those present at the beginning and transiently throughout the simulation, are summarized in Fig. 3 and further discussed in later sections.

A second BD-TMD salt-link exists in the nicotinic $\beta2$ subunit, from the full-EM template between n-β2-D271 on the M2–M3 loop (top of TMD) and n-β2-R46 on the $\beta1$–$\beta2$ loop (base of BD). The presence of a second salt bridge between the BD and the TMD in the n-$\beta2$ subunit may add rigidity to that β-subunit versus the α-subunit, although this acidic residue in the 271 position is not at all well conserved. This n-β2-D271-R46 salt-link is constantly flickering on and off throughout the simulation, with R46 also contacting n-α4-D/β2-E132.

Comparing the results from our models and MD simulations with the available experimental data, one can see that the models generated from the full-EM template better serve

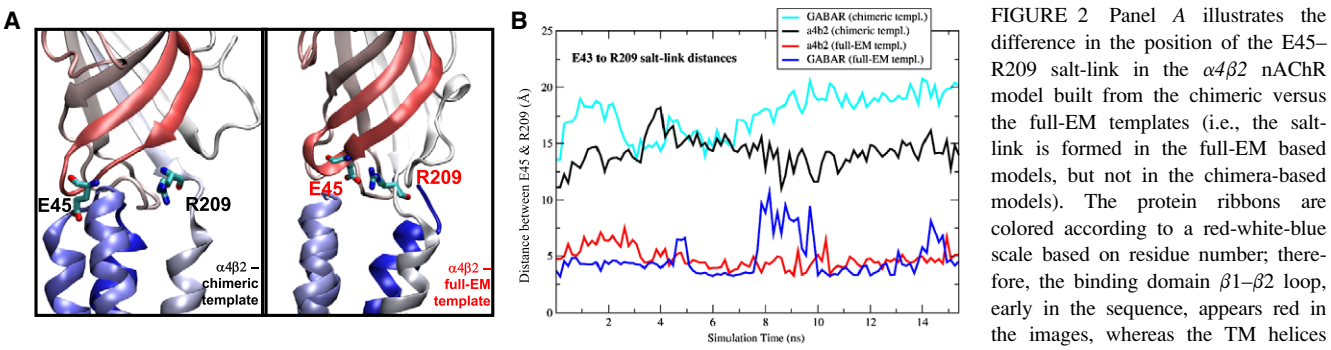

FIGURE 2 Panel *A* illustrates the difference in the position of the E45–R209 salt-link in the *$\alpha4\beta2$* nAChR model built from the chimeric versus the full-EM templates (i.e., the salt-link is formed in the full-EM based models, but not in the chimera-based models). The protein ribbons are colored according to a red-white-blue scale based on residue number; therefore, the binding domain $\beta1$–$\beta2$ loop, early in the sequence, appears red in the images, whereas the TM helices appear as darkening shades of blue. (*B*) A plot showing the side-chain center of mass (COM) distance between four E45 and R209 pairings in the four simulations. Salt-links were selected with a 3.2 Å cutoff between N-O atoms, but the side-chain COM is plotted to reduce noise in the plot. E45–R209 are bridged to each other in the EM-template model, but not in the chimeric-template models. For the chimeric-template based models, these two plot lines are representative of the typical lack of this salt-link in all the subunits within these two models (shown here for an nAChR α-subunit and a GABA β-subunit). In the EM-template-based models, the salt-link exists in all the subunits where the residues are conserved. Three of these E45–R209 salt-links, in the EM-template model subunits (two GABA β subunits and one nAChR α-subunit; the one shown here is from the GABA β-subunit) demonstrate a temporary switching whereby other nearby ionizable residues act as surrogate salt-bridge partners, and in this case switch back again.

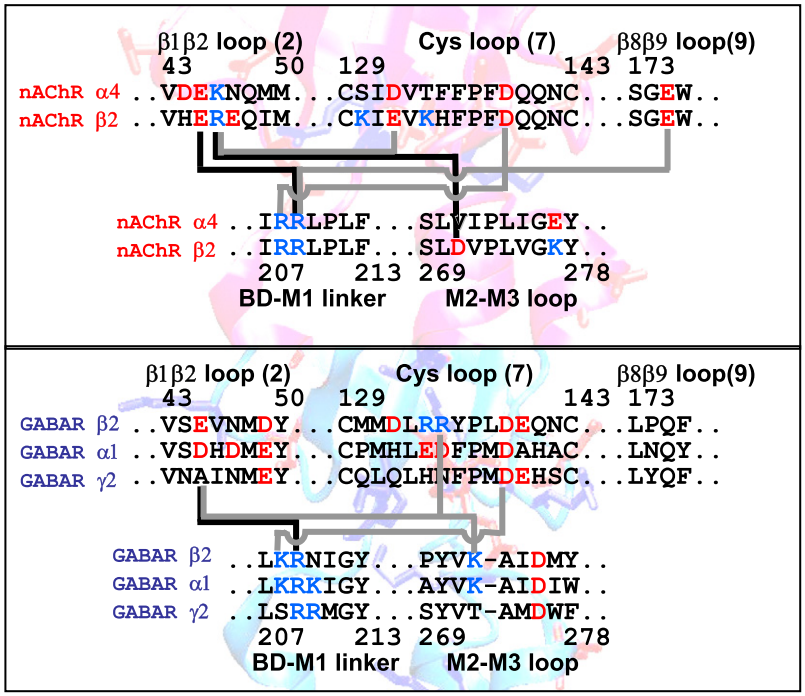

FIGURE 3 Network of potential salt-links exists at the interface between the LBD and TMD, involving the five loop sections of the structure that exist there in the models. The residue numbering is for the nicotinic α-subunit, and is kept consistent across the sequence alignment for clarity in making comparisons between the different structures. The black connecting lines show a salt-link present for >50% of the simulation, and the gray connecting lines indicate transient salt-links that are present for <50% of the simulation. E45–R209 is the longest lived of these salt-links and the best conserved across the CL-LGIC family. In the nAChR model, R209 transiently switches to E175. In GABAR, E/D45 transiently switches to either R136 or K272. Within the β-subunits of nAChR, an extra salt-link exists between R46 and D271, with R/K46 transiently forming a link to E/D132. R/K208–D139 in the nAChR and GABAR subunits represents another potentially conserved salt-link that is seen transiently in the simulations. Many of the charged residues at the interface are unpaired.

to represent the channel structure than those obtained using the chimeric template built from an EM TMD and an x-ray crystallographic BD structure. Hereafter, the discussion will focus solely on the simulations involving the nAChR $\alpha4\beta2$ and GABAR structures derived from the full-EM template.

Switching of the E45–R209 intrasubunit salt-link

Switching of the E45–R209 salt-link can be observed in both the nAChR and GABAR simulations. This is illustrated for the E45–R209 link in one of the β-subunits in the full-EM GABAR model (Fig. 2 *B*). In this context, the term ''switching'' refers to one or both of the side chains transiently linking to a different side chain, thereby temporarily breaking this E45–R209 salt-link. This switching can be observed to occur in three of the nine E/D45–R209 salt-bridges in the two models (there is no E/D in the GABAR $\gamma2$ subunit)—twice in GABAR (the two $\beta2$ subunits) and once in nAChR $\alpha4$ subunit. In the $\alpha4\beta2$ case, the n-$\alpha2$-E175 side chain on the $\beta8$–$\beta9$ loop competes with E45 for the R209 link, which is the dominantly observed pair in the chimeric template form of the model. This switching from R209's partner from n-E45 to n-E175 could be a vital transition step in the switching of states within the receptor. The E45 in the β-subunits of $\alpha4\beta2$ can also switch to n-$\beta2$-H135 on the Cys loop, but this weaker salt-bridge is not available in the α-subunits. In all three E45–R209 switching events, the salt-link transiently breaks and then reforms again after a few nanoseconds, as with the GABA β-subunit link illustrated in Fig. 2 *B*.

The GABAR model does not have an equivalent acidic residue to nAChR E175, and therefore the E45 switching, as seen in the two β-subunits, instead switches to either R135 in the Cys loop or g-$\beta2$/$\alpha1$-K272 on the M2–M3 loop. Of interest, this K272 (K275) residue was previously deemed to be important for the gating of the GABAR receptor on the basis of double-mutant experiments (25). In the GABAR α-subunit, the D45 residue can be seen switching off g-$\alpha1$-R209 to go to R126 in the Cys loop. Such slight differences in the important interface salt-link pairs between receptor isoforms and different members of the Cys-loop family may be vital in determining the nuances of gating kinetics that are so important for physiological channel function. In the GABAR $\gamma2$ subunit, the equivalent to R126 is an aspartate, and the E45 is changed to an alanine; therefore, no such salt-link can form. In fact, the GABAR $\gamma2$ subunit is the only subunit in the whole study that does not contain the R209–E45 salt-link. Whereas the nAChR β-subunit interface is more rigid because it is the only subunit with two salt-links, the GABAR γ-subunit BD-TM interface is more flexible because it contains no crossing salt-link at all. It is worth noting that the nearby E49 is present in the GABAR γ-subunit, but it is on the other side of the $\beta1$–$\beta2$ loop, points into the channel, and does not form an intersubunit salt-link throughout the simulation.

Other salt-bridges around the BD-TMD interface region observed in simulation

Several studies have suggested that, in addition to the E45–R209 link, other residues around the interface between the BD and TMDs appear to be important for transmitting the bound ligand signal to the TMD (24,25,43). As shown by previous simulations (26) and correlated motions seen in a

previous normal-mode analysis of nicotinic α7 (44), the interactions of loops at the interface (i.e., interactions between the M2–M3 loop, the Cys loop, the β1–β2 loop, and the linker between the BD and TMD at the top of M1) appear to be important for function. The construction of an AChBP-5HT$_3$ chimera required residues at the interface to be mutated to create a functional unit (43). A proline residue on the M2–M3 loop, near this salt-link, is also required for gating in 5HT$_3$ and nAChR receptors (24), although it is not completely conserved and is not present in all GABAR subunits. The dynamic interactions observed in the simulations reported here expand on the view of these interactions, especially for seemingly important salt-links.

At the nAChR BD-TMD interface, three conserved basic residues (R/K46, R208, and R209) and four conserved acidic residues (E45, D/E132, D139, and E175; Fig. 3) are present in all the subunits. Other less well-conserved charged side chains in some subunits include D44 and E277 (in α4), and E47, K130, K134, D272, and K277 (in β2). In fact, the β2 subunit has five unconserved charged residues at the interface, versus two in α4, again suggesting that perhaps the β-subunit interface is designed to be more rigid. Acidic/basic residues at the nAChR BD-TMD interface (other than E45–R209) form only transient salt-links during the simulation. In the initial structure, n-α4-D139, a completely conserved residue throughout the family, appears to have no salt-link partner, but transiently partners with R208 during the simulation. Yet, n-α4-R208 remains mostly unpartnered throughout the simulation, across all subunits, and is seen pointing into solution or the lipid headgroup region. E277 (nAChR.α4, which is not well conserved and is a lysine in the nAChR β-subunits) also does not have a salt-bridge partner and would not have one without a considerable conformational change in the structure; therefore, E277 spends much of the simulation interacting with water molecules and lipid headgroups. D132 (Cys loop, nAChR.α4; E132 in nAChR.β2) is usually unpartnered, but can be seen to transiently form links to β2-K/α4-R46 during the simulation. In the initial structure, β2-R/α4-K46 on the β1–β2 loop looks capable of forming an intersubunit salt-link with E175 in the β8–β9 loop, and it does so in one β4-α2 subunit interface (discussed further below). R/K46 also forms transient salt-links within the same subunit (to D132, D44 in α4, or E45 in β2).

In GABAR, there is again a complex network of potential salt-links, some of which form transiently during the simulation (Fig. 3). Other than the E45–R209 residues discussed above, there are other reasonably well-conserved acidic residues (E/D49, D139, and D276) and two basic lysines (K208 and K272). K208 is in both the β- and α-subunits, but not in the γ-subunit, and K272 is in just the β-subunit. As discussed above, K272 (along with R135) forms very transient links to the conserved E45, in the β-subunit only, when it is not linked to R209. D/E49, on the β1–β2 loop, does not form an interface salt-link; instead, it finds a strong interaction with K96 within the LBD. In a scheme similar to that observed in the nicotinic receptor, D139 and K208 are largely unpaired and face into solution, but do transiently interact with each other in some of the subunits. D276 does not appear to have a salt-link partner in any of the GABA subunits and points outward in solution.

A host of charged residues that are not so well conserved transiently act as salt-link partners with the conserved residues, including a pair of arginines that are only in the GABAR β-subunit and their equivalent acidic residues (Glu-Asp) in the α-subunit. Neither of these acidic residues have equivalent residues in the γ-subunit. In the β-subunits, R135 forms transient links to E45. The g-β2-R210 residue, neighbor to the conserved R209, faces away from the interface and forms an intersubunit salt-bridge with E168, which is on the β8-sheet just before the β8–β9 loop (discussed further below).

These transient links in both receptor types are most intriguing. They are suggestive of a mechanism whereby the receptor undergoes conformational shifts that are then stabilized and/or limited by defined positions as controlled by these salt-links. The unconserved residues may then offer modulation of these effects to provide subunit-specific gating properties.

Relative subunit motions and intersubunit links

Given the subunit rotations observed both experimentally (45) and computationally (26,44) that are consistent with the ''twist-to-open'' mechanism, one would expect strong intersubunit salt-links to restrict and/or modulate this motion, and therefore potentially be important for the functioning of the receptors. In accord with previous simulations and experiments, a 5–10° longitudinal-axis rotation was seen in the subunits in both the nAChR and GABAR simulations. Surprisingly, given the large number of charged residues in the LBDs of both receptor structures (and very few in the TMD), there are very few salt-links between the subunits that are either present in the initial models or form during the simulations. This illustrates that there are only a few points of connectivity within the complex. Mostly the structure has quite large gaps between subunits (both between BD and TMDs), which allows significant motion to take place. One site of connectivity is, of course, the ligand-binding site, which involves two subunits in each case. The lack of connectivity between subunits elsewhere may then allow ligand binding to have dramatic affects on how the subunits interact with each other, and bring about the rotation bias in motion that is necessary for gating to take place. More salt-links between subunits might have the effect of limiting the motion of the receptor and not allowing it to gate. There are several salt-links at the cytoplasmic mouth (near the BD-TMD interface), suggesting that this region is more of a hinge point, relative to the rotations and breathing required in the rest of the structure.

There are several transient salt-links at the very outer fringe of the BD, but very few in between that and the TMD. In both nAChR and GABAR, a salt-link forms between the M2

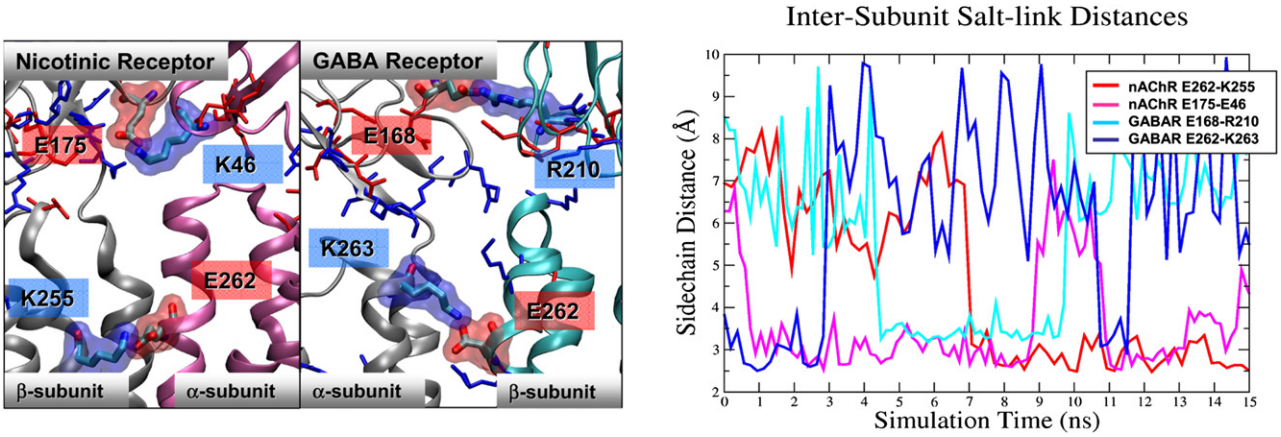

FIGURE 4 Only a small number of intersubunit salt-links appear to exist in the initial models or to even form during the simulation. In the nAChR BD, the salt-link between E175(β) and K46(α) seems to be equivalent to the salt-link E168(α) to R210(β) in the GABAR. On the pore-lining M2 helices of the TMDs, the link from K255(β) to E262(α) in the nAChR seems to be equivalent to the link from K263(α) to E262(β) in the GABAR. These salt-links are not present throughout the simulation. The graph in the lower panel shows their transient nature.

helices. In nAChR, two nonconserved residues (n-α4.E262 and n-β2.K255) interact with each other in intersubunit salt-links (Fig. 4). In GABAR, the equivalent residues (spatially) are g-β2.E262 and g-α1.K263 (Fig. 4). In the example shown in the plot in Fig. 4, this salt-link is not present in the initial structure but forms halfway through the simulation, with relatively small motions of the two side chains, and is present at all the interfaces. In GABAR, there is more competition with other residues in the other subunits and for intrasubunit links, and therefore the link is very transient. These residues are at the top of the pore-lining M2 helix, and this may be an important point of transmission of the gating motion from the α- to β-subunits. Even though these residues are not well conserved in the usual sense, it appears that for many common subunit combinations, and for both nAChR and GABAR, this salt-link will be conserved in the sequence and is seen in the models and the simulation.

A second potentially important intersubunit salt-link forms between β2 and α1 subunits in the GABAR, involving R210 on the β-subunit M1-linker by snorkeling away from the BD-TMD interface region and forming an intersubunit salt-bridge with E168, which is on the β8-sheet just before the β8–β9 loop (Fig. 4) in the GABA α1 subunit. This arginine is not conserved across the family of receptors and is only present in the GABAR-β subunits. However, the relative spatial position of this salt-link is very similar to a salt-link that forms between two residues conserved within the nAChR subunits: K46 on the β1–β2 loop of α-subunit, and E175 in the β8–β9 loop of the adjacent β-subunit (Fig. 4). This salt-link, as with the other intersubunit links, is consistently present throughout the simulation other than when E175 switches to form a transient link to K209 (as discussed above). The potential for its formation is then clearly demonstrated by the simulation. We postulate that this is an important salt-link within the structure, and we hope it can be tested experimentally.

In the α4β2 (EM-template) simulation, salt-links actually form between residues in the vestibule helix and residues at the cytoplasmic side of the receptor subunits, but since this helix is undergoing such large conformational fluctuations in this relatively short simulation, it is not possible to say whether this is significant or even at all relevant.

Just before this work was submitted for publication, the structure of a prokaryotic Cys-loop-like LGIC, solved by x-ray crystallography to 3.3 Å resolution, was released (46). The sequence is only 16% similar to the eukaryotic forms of the receptor (and does not, for instance, include the di-cysteine in the ''Cys loop''), but it clearly has an extremely similar fold. The TMD is noticeably more tightly packed, albeit with a less well-packed M4. The BD-TM interface is then less tightly packed but has a similar-looking network of charged residues available for salt-linking. The E45–R209 link is not present even though the Arg and Glu look conserved (R198 and E30). They are just not linked in the structure, although it appears that they could become linked. These obvious differences indicate either a real evolutionary difference in the structure-function relationship within the complex, or somewhat of a crystal-packing artifact that remains after removal of native lipid from the system.

CONCLUSIONS

Template selection for the CL-LGIC family has been discussed previously for both GABAR (47) and nicotinic channels (18). The findings here extend the view that the AChBP is a functional analog of the binding domain of the full receptors (43). Although the model based on a chimeric structure can yield much biologically relevant information (26,44), there are structural differences in the available full receptor structure (17) that must be included in the model to reveal biologically important motions and interdomain residue interactions in MD simulations. In the models built from the

chimeric receptor, R209 forms a link to E175 on the Cys loop, instead of the experimentally important (23) E45 residues as seen in the full-EM template models and simulations. Arginines or histidines on the Cys loop could act as surrogates for E45. It may be that switching between these two acidic side chains (E45 and R175) is an important step in gating for the receptor, as salt-links switch between coupling and decoupling BD and TMD motion. For the purposes of this study, however, this lack of an E45–R209 salt-bridge was treated as a discrepancy in the models. Of course, our conclusions rely on the accuracy of the template structure, which, at 4 Å, could have several incorrectly located side chains.

A previous simulation study of a chimeric α7 nAChR model also demonstrated the importance of the Cys loop as a stator about which the TM bundle can rotate and pivot (26). Our simulations all confirm that assessment. The disulphide bond on that loop is necessary to give it the rigidity to perform the stator role. The interactions of the other components at the BD-TM interface then become vital in modulating the rotation and pivot motions that contribute to gating.

The results and discussion have focused on salt-links within the structure, as these are potentially important interactions. However, the exact location of ionizable residues determines the actual strength of such salt-links. If it is accessible by solution, the salt-link can be quite weak (49), but if buried in a hydrophobic core, it can be as strong as -4 kcal/mol (50). The stabilization energy from the seemingly important E45–R209 link (and also D271–R45 in nicotinic β2) may be < -4 kcal/mol, as the simulation demonstrates that this salt-link has surrogates in the form of nearby ionizable residues, making the cost of breaking the link somewhat lower. Intersubunit links, such as E175–K46, appear to be water-accessible; therefore, they would be of lower strength but perhaps could allow faster conformational switching while still providing a shallow energy well for specific states of the receptor. It is likely that salt-links such as D271–R45 in nicotinic β2 that are not well conserved across the Cys-loop family, and appear to be transient and very fast switching in the simulation, may provide important gating modulatory differences that give rise to the subunit-specific kinetics of the different forms of the receptors. D139 is a completely conserved residue across the Cys-loop family, yet in the closed/desensitized state, around which these simulations were centered, it does not have an obvious role. Perhaps a transition to an open conformation would be partly stabilized by a salt-link to, for instance, R208 (as seen transiently in simulation) to the D139 residue.

Nonconserved salt-links may also have important implications for subunit-specific gating properties. For instance, the acidic residue on the M2–M3 loop in nAChR.α4 moves from the 277 position to the 271 position in nAChR.β2. In the β2 subunit, this acidic side chain has a long-lived salt-link to R46, but no such link can exist in the α-subunit. In fact, the 277 position switches from being acidic in the α4 subunit to being basic in the β2 subunit. One could argue that α4.E44 to β2.D47 is a similar switch.

The simulation study presented here also sheds more light on the mechanism of these channels. MD simulation can present possible motions, as seen here. Gating does not occur on the timescale of these simulations, nor should it, but the data show component motions that may contribute to gating. These component motions may be on the nanosecond timescale even though the complete gating reaction may take milliseconds due to the requirement to line up all of the necessary component motions. A mechanism was previously proposed (26) on the basis of multiple simulations, experimental structures, and biochemical studies (17,18,25). This mechanism has been expanded and modified by recent normal-mode modeling studies (44,51). The study presented here can help to further explain the potential gating scheme and relate the biochemical evidence to a mechanistic description. Multiple potential salt-links exist as part of a complex network of acidic and basic residues, very few of which are close enough in the models to form links in any single state of the receptor. The implication, therefore, is that different interdomain salt-links form at different points on the receptor activation cycle. The key extension to the gating model, then, as described here, is that the BD–TMD salt-links do not necessarily couple binding of the agonist to gating directly, but may act as a set of limits on the motions possible within the subunit. The biasing of these limits could be altered by the binding of either the agonist or allosteric regulator molecules such as anesthetics.

SUPPORTING MATERIAL

Sequences are available at http://www.biophysj.org/biophysj/supplemental/S0006-3495(09)01220-X.

This work was supported by the Laboratory Directed Research and Development Program (grant 05-ERD-025) at Lawrence Livermore National Laboratory, and performed under the auspices of the U.S. Department of Energy by the Lawrence Livermore National Laboratory under contract DE-AC52-07NA27344. UCRL#: UCRL-JRNL-231445.

REFERENCES

1. Karlin, A., and M. H. Akabas. 1995. Toward a structural basis for the function of nicotinic acetylcholine receptors and their cousins. *Neuron*. 15:1231–1244.
2. Changeux, J. P., and A. Taly. 2008. Nicotinic receptors, allosteric proteins and medicine. *Trends Mol. Med.* 14:93–102.
3. Whiting, P. J. 2003. The GABAA receptor gene family: new opportunities for drug development. *Curr. Opin. Drug Discov. Devel.* 6:648–657.
4. Walters, R. J., S. H. Hadley, K. D. Morris, and J. Amin. 2000. Benzodiazepines act on GABAA receptors via two distinct and separable mechanisms. *Nat. Neurosci.* 3:1274–1281.
5. Milligan, C. J., N. J. Buckley, M. Garret, J. Deuchars, and S. A. Deuchars. 2004. Evidence for inhibition mediated by coassembly of GABAA and GABAC receptor subunits in native central neurons. *J. Neurosci.* 24:7241–7250.
6. Baumann, S. W., R. Baur, and E. Sigel. 2002. Forced subunit assembly in $\alpha1\beta2\gamma2$ GABAA receptors. Insight into the absolute arrangement. *J. Biol. Chem.* 277:46020–46025.

7. Amin, J., and D. S. Weiss. 1993. GABAA receptor needs two homologous domains of the β-subunit for activation by GABA but not by pentobarbital. *Nature*. 366:565–569.
8. Hansen, S. B., G. Sulzenbacher, T. Huxford, P. Marchot, P. Taylor, et al. 2005. Structures of Aplysia AChBP complexes with nicotinic agonists and antagonists reveal distinctive binding interfaces and conformations. *EMBO J*. 24:3635–3646.
9. Arias, H. R., P. Bhumireddy, and C. Bouzat. 2006. Molecular mechanisms and binding site locations for noncompetitive antagonists of nicotinic acetylcholine receptors. *Int. J. Biochem. Cell Biol*. 38:1254–1276.
10. Papke, R. L., and R. E. Oswald. 1989. Mechanisms of noncompetitive inhibition of acetylcholine-induced single-channel currents. *J. Gen. Physiol*. 93:785–811.
11. Coates, K. M., and P. Flood. 2001. Ketamine and its preservative, benzethonium chloride, both inhibit human recombinant α7 and $\alpha4\beta2$ neuronal nicotinic acetylcholine receptors in *Xenopus* oocytes. *Br. J. Pharmacol*. 134:871–879.
12. Gumilar, F., H. R. Arias, G. Spitzmaul, and C. Bouzat. 2003. Molecular mechanisms of inhibition of nicotinic acetylcholine receptors by tricyclic antidepressants. *Neuropharmacology*. 45:964–976.
13. Blanton, M. P., E. A. McCardy, and M. J. Gallagher. 2000. Examining the noncompetitive antagonist-binding site in the ion channel of the nicotinic acetylcholine receptor in the resting state. *J. Biol. Chem*. 275:3469–3478.
14. Law, R. J., C. Capener, M. Baaden, P. J. Bond, J. Campbell, G. Patargias, et al. 2005. Membrane protein structure quality in molecular dynamics simulation. *J. Mol. Graph. Model*. 24:157–165.
15. Fan, A., and A. E. Mark. 2003. Relative stability of protein structures determined by x-ray crystallography or NMR spectroscopy: a molecular dynamics simulation study. *Proteins*. 52:111–120.
16. Bartels, C., M. Schaefer, and M. Karplus. 1999. Determination of equilibrium properties of molecular systems using multidimensional adaptive importance sampling. *J. Chem. Phys*. 111:8048–8067.
17. Unwin, N. 2005. Refined structure of the nicotinic acetylcholine receptor at 4A resolution. *J. Mol. Biol*. 346:967–989.
18. Sine, S. M., and A. G. Engel. 2006. Recent advances in Cys-loop receptor structure and function. *Nature*. 440:448–455.
19. Ivanov, I., X. Cheng, S. M. Sine, and J. A. McCammon. 2007. Barriers to ion translocation in cationic and anionic receptors from the Cys-loop family. *J. Am. Chem. Soc*. 129:8217–8224.
20. Sansom, M., P. Bond, O. Beckstein, P. C. Biggin, J. Faraldo-Gómez, et al. 2002. Water in ion channels and pores—simulation studies. *Novartis Found. Symp*. 245:66–78.
21. Reference deleted in proof.
22. Mukhtasimova, N., and S. M. Sine. 2007. An intersubunit trigger of channel gating in the muscle nicotinic receptor. *J. Neurosci*. 27:4110–4119.
23. Lee, W. Y., and S. M. Sine. 2005. Principal pathway coupling agonist binding to channel gating in nicotinic receptors. *Nature*. 438:243–247.
24. Lummis, S. C., D. L. Beene, L. W. Lee, H. A. Lester, R. W. Broadhurst, et al. 2005. *Cis-trans* isomerization at a proline opens the pore of a neurotransmitter-gated ion channel. *Nature*. 438:248–252.
25. Xiu, X., A. P. Hanek, J. Wang, H. A. Lester, and D. A. Dougherty. 2005. A unified view of the role of electrostatic interactions in modulating the gating of Cys loop receptors. *J. Biol. Chem*. 280:41655–41666.
26. Law, R. J., R. H. Henchman, and J. A. McCammon. 2005. A gating mechanism proposed from a simulation of a human α7 nicotinic acetylcholine receptor. *Proc. Natl. Acad. Sci. USA*. 102:6813–6818.
27. O'Mara, M., B. Cromer, M. Parker, and S. H. Chung. 2005. Homology model of the GABAA receptor examined using Brownian dynamics. *Biophys. J*. 88:3286–3299.
28. Cheng, X., H. Wang, B. Grant, S. M. Sine, and J. A. McCammon. 2006. Targeted molecular dynamics study of C-loop closure and channel gating in nicotinic receptors. *PLOS Comput. Biol*. 2:e134.
29. Brejc, K., W. J. van Dijk, and R. Klaassen. 2001. Crystal structure of an ACh-binding protein reveals the ligand-binding domain of nicotinic receptors. *Nature*. 411:269–276.
30. Miyazawa, A., Y. Fujiyoshi, and N. Unwin. 2003. Structure and gating mechanism of the acetylcholine receptor pore. *Nature*. 423:949–955.
31. Jansen, M., and M. H. Akabas. 2006. State-dependent cross-linking of the M2 and M3 segments: functional basis for the alignment of GABAA and acetylcholine receptor M3 segments. *J. Neurosci*. 26:4492–4499.
32. Mercado, J., and C. Czajkowski. 2006. Charged residues in the α1 and β2 pre-M1 regions involved in GABAA receptor activation. *J. Neurosci*. 26:2031–2040.
33. Sánchez, R., and A. Sali. 1997. Evaluation of comparative protein structure modeling by MODELLER-3. *Proteins*. 1(Suppl.):50–58.
34. MacKerrell, A. D., A. D. Mackerell, and C. L. Brooks. 1998. All-atom empirical potential for molecular modeling and dynamics studies of proteins. *J. Phys. Chem. B*. 102:3586–3616.
35. Phillips, J. C., R. Braun, W. Wang, J. Gumbart, E. Tajkhorshid, et al. 2005. Scalable molecular dynamics with NAMD. *J Comput. Chem*. 26:1781–1802.
36. Humphrey, W., A. Dalke, and K. Schulten. 1996. VMD: visual molecular dynamics. *J. Mol. Graph*. 14:33–38.
37. Grubmuller, H., B. Heymann, and P. Tavan. 1996. Ligand binding: molecular mechanics calculation of the stratavidin-biotin rupture force. *Science*. 271:997–999.
38. Ryckaert, J. P., G. Ciccotti, and H. J. C. Berendsen. 1977. Numerical integration of the Cartesian equations of motion of a system with constraints: molecular dynamics of n-alkanes. *J. Comput. Phys*. 23:327–342.
39. Jorgensen, W. L., J. Chandrasekhar, J. D. Madura, R. W. Impey, and M. L. Klein. 1983. Comparison of simple potential functions for simulating liquid water. *J. Chem. Phys*. 79:926–935.
40. Smart, O. S., J. G. Neduvelil, X. Wang, B. A. Wallace, and M. S. Sansom. 1996. Hole: a program for the analysis of the pore dimensions of ion channel structural models. *J. Mol. Graph*. 14:354–360.
41. Van Der Spoel, D., E. Lindahl, B. Hess, G. Groenhof, A. E. Mark, et al. 2005. GROMACS: fast, flexible, and free. *J. Comput. Chem*. 26:1701–1718.
42. DeLano, W. L. 2002. The PyMOL molecular graphics system. http://www.pymol.org.
43. Bouzat, C., F. Gumilar, G. Spitzmaul, H. L. Wang, D. Rayes, et al. 2004. Coupling of agonist binding to channel gating in an ACh-binding-protein linked to an ion channel. *Nature*. 430:896–900.
44. Cheng, X., B. Lu, B. Grant, R. J. Law, and J. A. McCammon. 2006. Channel opening motion of α7 nicotinic acetylcholine receptor as suggested by normal mode analysis. *J. Mol. Biol*. 355:310–324.
45. Unwin, N. 2003. Structure and action of the acetylcholine receptor explored by electron microscopy. *FEBS Lett*. 555:91–95.
46. Hilf, R., and R. Dutzler. 2008. X-ray structure of a prokaryotic pentameric ligand-gated ion channel. *Nature*. 452:375–380.
47. Ernst, M., S. Bruckner, S. Boresch, and W. Sieghart. 2005. Comparative models of GABAA receptor extracellular and transmembrane domains: important insights in pharmacology and function. *Mol. Pharmacol*. 68:1291–1300.
48. Reference deleted in proof.
49. Serrano, L., A. Horovitz, B. Avron, M. Bycroft, and A. R. Fersht. 1990. Estimating the contribution of engineered surface electrostatic interactions to protein stability by using double-mutant cycles. *Biochemistry*. 29:9343–9352.
50. Wimley, C. W., and S. H. White. 1996. Experimentally determined hydrophobicity scale for proteins at membrane interfaces. *Nat. Struct. Biol*. 3:842–848.
51. Taly, A., M. Delarue, T. Grutter, M. Nilges, N. Le Novère, et al. 2005. Normal mode analysis suggests a quaternary twist model for the nicotinic receptor gating mechanism. *Biophys. J*. 88:3954–3965.